Title: Efficient and Tunable Phosphorescence of new Platinum(II) Complexes Based on the Donor-π-Acceptor Schiff bases

Author: Jie Zhang Guoliang Dai Fengshou Wu Dan Li Dongchun Gao Haiwei Jin Song Chen Xunjin Zhu Chenxiu Huang Deman Han

PII: S1010-6030(15)00371-8
DOI: http://dx.doi.org/doi:10.1016/j.jphotochem.2015.09.018
Reference: JPC 10018

To appear in: *Journal of Photochemistry and Photobiology A: Chemistry*

Received date: 24-5-2015
Revised date: 18-9-2015
Accepted date: 29-9-2015

Please cite this article as: Jie Zhang, Guoliang Dai, Fengshou Wu, Dan Li, Dongchun Gao, Haiwei Jin, Song Chen, Xunjin Zhu, Chenxiu Huang, Deman Han, Efficient and Tunable Phosphorescence of new Platinum(II) Complexes Based on the Donor-*rmpi*-Acceptor Schiff bases, Journal of Photochemistry and Photobiology A: Chemistry http://dx.doi.org/10.1016/j.jphotochem.2015.09.018

ARTICLE

Efficient and Tunable Phosphorescence of new Platinum(II) Complexes Based on the Donor-π-Acceptor Schiff bases

Jie Zhang[a,b*] zhang_jie@tzc.edu.cn hdm@tzc.edu.cn, Guoliang Dai[c], Fengshou Wu[d] wfs42@126.com, Dan Li[e], Dongchun Gao[a], Haiwei Jin[a], Song Chen[f], Xunjin Zhu[f] xjzhu@hkbu.edu.hk, Chenxiu Huang[a], Deman Han[a]

[a]School of Pharmaceutical and Chemical Engineering, Taizhou University, 318000 Taizhou, P. R. China.
[b]Department of Chemical and Biological Engineering, Zhejiang University, 310027 Hangzhou, P.R. China.
[c]School of Chemistry, Biology and Materials Engineering, Suzhou University of Science and Technology, 215009 Suzhou, P. R. China.
[d]Key Laboratory for Green Chemical Process of the Ministry of Education, Wuhan Institute of Technology, Wuhan, P. R. China.
[e]Department of Scientific Research, Taizhou University, 318000 Taizhou, P. R. China
[f]Department of Chemistry and Institute of Advanced Materials, Hong Kong Baptist University, Waterloo Road, Hong Kong, P.R. China.
[*]Corresponding author.

Graphical abstract

The condensation of 4-(diethylamino)-2-hydroxybenzaldehyde with 2,3-diaminomaleonitrile and benzene-1,2-diamine, respectively, afforded two donor-π-acceptor Schiff base ligands **H_2L^1** and **H_2L^2**. And their corresponding platinum(II) complexes **PtL^1**, **PtL^2** show yellow to red emissions with the highest quantum yield of 8.6% for **PtL^1**.

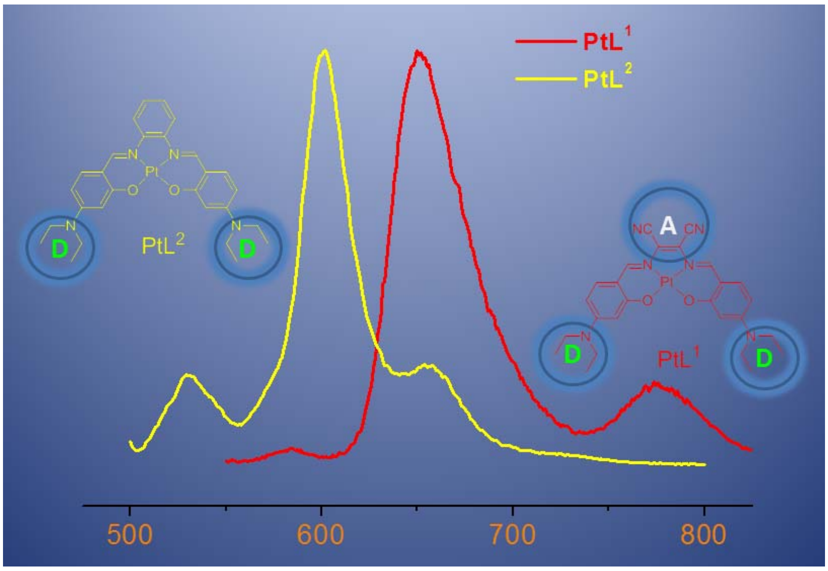

Highlights

1) Donor-π-acceptor type platinum(II) Schiff base complexes were developed.

2) Their photophysical properties and electrochemical behaviors were investigated.

3) The HOMO and LUMO energy levels can be adjusted by the structure optimization.

4) The complexes emit in the range of yellow to red.

5) Their photophysical properties were investigated by density functional theory.

Abstract

The condensation of 4-(diethylamino)-2-hydroxybenzaldehyde with 2,3-diaminomaleonitrile and benzene-1,2-diamine, respectively, afforded two donor-π-acceptor Schiff base ligands **H_2L^1** and **H_2L^2**. For comparison, the condensation of 3,5-di-*tert*-butyl-2-hydroxybenzaldehyde with 4-(trifluoromethyl)benzene-1,2-diamine produced the ligand **H_2L^3**. Subsequently, their corresponding platinum(II) complexes **PtL^1**, **PtL^2** and **PtL^3** were prepared through the metallation of ligands with K_2PtCl_4. All the ligands and complexes were characterized by ^{1}H NMR, infrared spectroscopy and mass spectrometry. And their thermal stabilities, photophysical properties, and electrochemical behaviors were investigated in detail. These complexes show yellow to red emissions with the highest quantum yield of 8.6% for **PtL^1**. The decay times in microsecond scale (1.97-2.35 μs) indicate their phosphorescence characteristics arising from the triplet state. The B3LYP density functional theory calculations shows that the HOMO-LUMO gaps of **PtL^1**, **PtL^2** and **PtL^3** are 2.53, 3.07 and 2.78 eV, respectively, which are well consistent with their photophysical properties. With the advantages of preparative accessibility and high thermal stability, these new phosphorescent platinum(II) complexes are attractive as emissive layer in organic light-emitting diodes.

Transition metal complexes of N_2O_2 Schiff base derived from salicylaldehyde and diamines have attracted considerable interest as a promising class of luminescent materials with the advantages of preparative accessibility and thermal stability.[1] Typically, the metal complexation leads to the formation of geometrically constrained acentric, generally planar structural Schiff base complexes with an enhanced emission in comparison with their related free ligands. Amongst them, zinc Schiff base complexes have been widely investigated.[2] Our group previously reported several donor-π-acceptor zinc(II) and nickel(II) Schiff base complexes which possess two-photon induced fluorescence (TPIF). [3] Since these zinc complexes can only emit in a singlet state with low quantum yield efficiency, some heavy metal Schiff base complexes such as Pt(II), Ir(III), Au(I) *et al.* have been developed with enhanced intersystem crossing (ISC) due to the strong spin-orbit coupling, which overcomes the limitation of 25% efficiency of conventional fluorescent OLEDs with the nature of emission from pure singlet excitons.[4] In general, both singlet and triplet excitons formed with the ratio of 1:3 under electrical excitation, therefore, contribute the light emission by the fast exciton energy transfer in phosphorescent organic light-emitting diodes (PhOEDs) based on the heavy metal complexes, potentially resulting in a 100% quantum yields. Currently, phosphorescent materials with triplet state emission have been widely and successfully applied in organic light-emitting diodes (OLEDs) fabrication.[5]

Among those heavy metal complexes, phosphorescent platinum(II) complexes have been well studied by Thompson, Forrest, Che and coworkers.[6] Compared with the most reported iridium complexes, platinum complexes have some different characteristics: (1) square planar structure with four coordination; (2) rich photophysical properties suitable for OLEDs, sensor, organic photovoltaic (OPV) *et al.*; (3) existing Pt…Pt and π-π interactions with adjustable emission wavelength and efficiency; (4) lower HOMO and higher LUMO level with better electron injecting and transporting. Specifically, Che and his coworkers have devoted much effort in platinum(II) Schiff base complexes,[7] which show strong triplet state emissions with high quantum efficiency. In these platinum(II) Schiff base complexes, it was found that the formation of aggregate/excimer would reduce the emission efficiency and also affect the color purity at their high concentrations. This is mainly attributed to the triplet-triplet annihilation, Pt…Pt and π-π interactions at the high concentration in solid state. In our previous work, a series of new symmetric and asymmetric platinum(II) Schiff base complexes with bulky substituents such as *tert*-butyl and triphenylamino groups, have also been developed, leading to a high efficiency in OLED devices due to effectively suppressing of the aggregation or excimer formation.[8]

In this contribution, three Schiff base ligands derived from the condensation of 4-(diethylamino)-2-hydroxybenzaldehyde with 2,3-diaminomaleonitrile, and benzene-1,2-diamine, respectively, or 3,5-di-*tert*-butyl-2-hydroxybenzaldehyde with 4-(trifluoromethyl)- benzene-1,2-diamine. Subsequently, their platinum(II) complexes were prepared and characterized. The strong electron withdrawing units involved in the complexes such as dicyanovinyl and (trifluoromethyl)phenyl, and electron donating units such as 4-diethylaminophenyl and 3,5-di-*tert*-butyl-phenyl can finely tune the emission wavelength from yellow to red and somewhat improve the emission efficiency.[9] With the advantages of preparative accessibility and high thermal stability, these new phosphorescent platinum(II) complexes are attractive as emissive materials in OLEDs.

Results and Discussion

Synthesis

The Schiff base ligands (**H_2L^1–H_2L^3**) were prepared via the condensation of the substituted 2-hydroxybenzaldehydes with diamines according to the traditional method (Scheme 1).[10] Then the ligands were reacted with potassium tetrachloroplatinate(II) and KOH in DMF at 70℃ to give the corresponding platinum(II) Schiff base complexes. These complexes **PtL^1**, **PtL^2** and **PtL^3** show good solubility in common organic solvents. All the new Schiff base ligands and platinum(II) complexes were characterized by ^{1}H NMR, infrared spectroscopy (IR), mass spectrometry (MS), UV-visible spectrum and elemental analysis.

Characterization of the ligands and complexes

The ^{1}H NMR spectra of the Schiff base ligands **H_2L^1**, **H_2L^2** and **H_2L^3** in $CDCl_3$ exhibit a board singlet peak at 12.49, 13.63 and 13.28 ppm for the O–H protons, respectively. The chemical shift is typical for the resonance-assisted hydrogen bonded (RAHB) proton of O–H…N=C. Another characteristic sharp singlet peaks appear at 8.57, 8.42 and 8.67 ppm for imino protons of the ligands **H_2L^1**, **H_2L^2** and **H_2L^3**, respectively. The ^{1}H NMR spectra of their platinum(II) complexes **PtL^1**, **PtL^2** and **PtL^3** in $CDCl_3$ similarly exhibit a singlet peak at δ 8.31, 8.98 and 8.89 ppm for the imino protons, respectively. All the new compounds were further characterized by IR and MS. The IR absorption peak for the ligands and complexes between 1616–1636 cm^{-1} can be assigned as the C=N stretching vibrations. The MALDI-TOF-MS spectra of the three platinum(II) complexes exhibit $[M]^+$ or $[M+H]^+$ peaks with values less than 5 ppm deviation from the theoretical ones.

UV-visible absorption of the ligand and complexes

The Schiff base ligands **H_2L^1**, **H_2L^2** and **H_2L^3** exhibit UV-visible absorption spectra between 200–600 nm (**Figure 1**), which can be assigned to intra-ligand π-π* and n-π* transitions. Specifically, the ligand **H_2L^1** shows a much red shifted absorption peak at 571 nm in comparison with **H_2L^2** and **H_2L^3**, which is consistent with the TD-DFT calculation data of the ligands, as shown in the **Table S1 and Figure S3-S5** (**ESI**). Obviously, the structure of **H_2L^1** is a donor-π-acceptor (D-π-A) type, leading to a very strong ligand-to-ligand charge transfer (LLCT) character. In contrast, the structure of **H_2L^2** and **H_2L^3** are donor-π (D-π) and acceptor-π (A-π) type, respectively, both characteristic of a relatively weak LLCT. As a result, the maximum absorption and emission peaks of D-π-A type compound locate at longer wavelengths than its D-π and A-π counterparts. Based on the DFT calculation data, those absorption peaks of the ligands between 400–600nm are mostly attributed to LLCT. On the other hand, three platinum(II) complexes show intense absorption bands in the range of 400–600 nm, which can be assigned to π-π* transitions of LLCT mixed with metal-to-ligand charge-transfer (MLCT) (**Figure 1**).[7c] This assignment is also supported by the DFT calculation data, as shown in **Figure 4** and **Table 3**, in which the lowest absorption energy bands of the platinum complexes are ranged in 500–600 nm, arising from MLCT and LLCT. Similarly, the maximum absorption peak of **PtL^1** is also red-shifted compared with **PtL^2** and **PtL^3**, due to its donor-π-acceptor structural characteristics. In our previous study of the Schiff base complexes, it was found that the HOMO mainly located on the phenolate fragments and metal ion while the LUMO located on the imino part.[3a] And the donor or acceptor groups at the 5-position of the phenolate fragments have little effect on the HOMO and LUMO energy levels. In contrast, the electron donating groups at 4-position of the phenolate fragments and the electron withdrawing groups at the imino in **PtL^1** results in a donor-π-acceptor configuration with efficient intramolecular charge transfer, which can effectively adjust the HOMO and LUMO energy levels.

Emission of the ligand and complexes

As shown in **Figure 2**，**Figure S1** (**ESI**) and **Table 1**, the emission spectra of the platinum(II) Schiff base complexes exhibit yellow to red emissions in the visible range of 531–776 nm. The platinum(II) complexes **PtL^1** modified by both electron-donating and electron-withdrawing groups show a much red shifted emission in comparison with **PtL^2** and **PtL^3** only with either electron-donating group or electron-withdrawing group. The quantum yields of the Schiff base complexes are moderate, from 0.87% to 8.6%, which are comparable with the reported values by our group[8] and Che's group[7]. The decay times in microsecond scale (1.97–2.35 μs) indicates the emission arise from the triplet state (**Figure S2**, **ESI**). The triplet state emission can be attributed to intraligand charge transfer and metal-to-ligand charge-transfer (MLCT). [7c]

Electrochemical Properties and Thermal Stability

The cyclic voltammetry behaviour of platinum(II) Schiff base complexes have been examined. Cyclic voltammetry study can give fundamental information on the number of oxidation/reduction processes and the redox potentials of the compounds. Furthermore, the HOMO-LUMO energy gap can be estimated from its redox potentials. Cyclic voltammetry behaviors of the platinum(II) Schiff base complexes were recorded in degassed acetonitrile with 0.1 M tetrabutylammonium hexafluorophosphate as supporting electrolyte at a scan rate of 50 mV s^{-1}. A glassy carbon electrode was used as working electrode, a platinum(II) wire was used as the auxiliary electrode with a Ag/Ag$^+$ as the reference electrode. The cyclic voltammogram of **PtL^1**, **PtL^2** and **PtL^3** is shown in **Figure 3,** and the electrochemical data of the three complexes are listed in **Table 2**. The irreversible anodic waves are attributed to the oxidation of Schiff base ligand.[7c] The onset of the first oxidation process of **PtL^1** occurs at about 0.35 V, and **PtL^2** at 0.29V, while **PtL^3** shows a more anodic potential with the onset of the first oxidation at about 0.71 V. Apparently, the electron releasing group of diethylamine at 4-position of the phenolate fragments accelerates the oxidation of **PtL^1** and **PtL^2**.[11] The LUMO-HOMO energy gap can be calculated by UV-vis absorption spectra. The energy gaps of these complexes are between 1.78–2.11 eV. Furthermore, the HOMO and LUMO energy levels of these complexes are estimated from the oxidation and energy gap [calculated according to the following equations: HOMO = $-(E_{ox} + 4.71)$ eV and LUMO = $(E_{gap}-\text{HOMO})$ eV] to be −5.42 to −5.06 eV and −3.50 to −3.28 eV, respectively. [12] The complex **PtL^1** shows a comparable HOMO level as **PtL^2**, but a much lower LUMO than **PtL^2** due to the electron deficient cyano substituents at imino part. Similarly, **PtL^3** exhibits a lower LUMO than **PtL^2** due to the electron withdrawing property of trifluoromethyl group at phenylene part.

The thermal stabilities of the complexes were investigated by thermogravimetric analysis (TGA) and differential scanning calorimetry (DSC) methods. As shown in **Table 2**, these complexes are thermally stable with decomposed temperatures as high as 352°C (**Table 2**).

Theoretical Calculation

The geometries of all the molecules were optimized by employing the B3LYP density functional theory method.[13] In the calculations, the 6-6-311++G** basis set was used for the C, H, O, N and F atoms, and the effective core potentials (ECP) of Stuttgart basis set was used for the platinum, the 6*s* and 5*d* in platinum atom were treated explicitly by a (8*s*7*p*6*d*) Gaussian basis set contracted to [6*s*5*p*3*d*].[14] The identification of the real minimum is ensured by harmonic vibrational frequency analysis of each of the optimized geometries. All the three complexes were in singlet ground states, and were calculated through direct minimization of the SCF energy. The major transitions based on the above structures were obtained by the time-dependent density functional theory (TD-DFT) by the B3LYP method with the same basis set. All calculations in this study were performed using the Gaussian 03 program.[15]

The optimized geometries of the complex **PtL^1**, **PtL^2** and **PtL^3** are shown in **Figure 4**, **Figure S6-S8 and Table S3-S5** (**ESI**). It is clear that the platinum center and the Schiff bases are coplanar in all these three compounds. The Natural Atomic Orbital (NBO) analysis[16] of the optimized geometries of the complexes indicate the platinum atom carries the positive charges, while both O and N carry the negative charges. Therefore, the two O atoms and two N atoms form a negative charges cavity, which is conducive to the coordination with metal platinum (**Table S2**).

The frontier orbital properties including the highest occupied molecular orbital (HOMO), the lowest unoccupied molecular orbital (LUMO) and nearby molecular orbitals can provide important information about the photophysical properties of a molecule. The stability of a complex is also closely related to the energy level and gap of HOMO and LUMO. The calculated HOMO-LUMO gaps of **PtL^1**, **PtL^2** and **PtL^3** were 2.53, 3.07 and 2.78 eV, respectively, which indicate they can be excited easily. All these data is consistent with the experiment results. The HOMOs mainly locate on the phenolate fragments and middle metal atom in the complexes. The HOMO (π orbital) was formed by p orbital of C, N and O and *d* orbital of platinum, which contain a few proportion *s* orbital (**Figure 5**). The LUMOs mainly locate on the imino part, which is composed by *p*-*π** orbital of C, N and O. The electrons transfer from phenolate fragments and middle metal to imino part when they are excited from the ground states to the excited states according to molecular orbital analysis. The **Figure 5** shows the electron cloud distributions and composition characteristics of the frontier molecular orbitals.

The electronic transitions of **PtL^1**, **PtL^2** and **PtL^3** were calculated by Time-Dependent B3LYP methods, and their wavelength and transition energies and oscillator strengths are listed in the **Table 3**. Take **PtL^2** as an example, HOMO is the π orbital composed of *p* orbital of C, N and *d* orbital of middle metal (**Figure 5**, **Table 3**), and the S1 transition originates from the transition of HOMO→LUMO (π→π*, LLCT and MLCT). The maximum UV-visible absorption wavelength of **PtL^2** was determined as 491 nm in experiment, which is consistent with the calculated value of 506 nm. And the S1 transition of **PtL^1** (550 nm), originated from the HOMO-1→LUMO (π→π*, LLCT and MLCT) transition, is obviously red shifted induced by the electron acceptor CN group. The *p* orbital of the N atoms of the CN groups was also involved in the LUMO orbital (π* orbital), leading to the delocalization of the orbital.

Conclusions

In this work, a series of donor-π-acceptor platinum(II) Schiff base complexes have been developed. These compounds were fully characterized by ^{1}H NMR, IR, MS, UV-visible absorption, elemental analysis. And the three complexes emit yellow to red light with the highest quantum yields of 8.6% for **PtL^1**. The decay times are in microsecond scale (1.97-2.35μs) indicating the triplet state characteristics of the emissions. The B3LYP density functional theory calculations show that the platinum center and the Schiff bases ligands were coplanar and the HOMO-LUMO gaps of **PtL^1**, **PtL^2** and **PtL^3** were calculated to be 2.53, 3.07 and 2.78 eV, respectively, which are well consistent with their photophysical properties. Benefiting from tunable emissions with high phosphorescent quantum yields, these platinum complexes are particularly interesting for OLEDs and OLEC applications.

Experimental Section

Materials and methods: The chemicals were purchased from Aladdin Reagent Company and used as received. Silica gel 60 (0.04–0.063 mm) for column chromatography was purchased from Qingdao Haiyang Chemical Co., Ltd. NMR spectra were recorded on a Bruker Ultrashield 400 Plus NMR spectrometer. High-resolution matrix-assisted laser desorption/ionization time-of-flight (MALDI-TOF) mass spectra were recorded with a Bruker Autoflex MALDI-TOF mass spectrometer. The C, H and N microanalyses were performed with a Carlo Erba 1106 elemental analyzer. The IR spectra were recorded with a Shimadzu IRAffinity-1 FTIR spectrometer as KBr disc. Thermogravimetrical studies were performed from 30 to 1000 °C at 10 °C/min under nitrogen on a TA Instruments SDTQ600 (TA instruments). Electronic absorption spectra in the UV-visible region were recorded on a Shimadzu UV-2450 UV/Vis spectrophotometer, steady-state visible fluorescence and PL excitation spectra on a FLS980 Photoluminescence Spectrometer (Edinburgh Instruments) and visible decay spectra on a pico-N$_2$ laser system (PTI TimeMaster) with λ_{exc} = 430 nm. Luminescence quantum yields (Φ_{em}) in degassed dichloromethane solution were determined with [Ru(bpy)$_3$](PF$_6$)$_2$ (bpy = 2,2'-bipyridine) in acetonitrile as a standard reference solution (Φ_{em} = 0.062). It was calculated by $\Phi_s = \Phi_r(B_r/B_s)(n_s/n_r)^2(D_s/D_r)$, where the subscripts r and s denote reference standard and the sample solution, respectively, and n, D, and Φ are the refractive index of the solvents, the integrated intensity, and the luminescence quantum yield, respectively. The quantity B is calculated by $B = 1\text{-}10^{-AL}$, where A is the absorbance at the excitation wavelength and L is the optical path length.

H$_2$L^1 To a stirred solution of 2,3-diaminomaleonitrile (63 mg and 0.58 mmol) in absolute ethanol (18 mL), 4-(diethylamino)-2-hydroxybenzaldehyde (450 mg and 2.33 mmol) was added. The resulting mixture was refluxed 12 hours. After cooling to room temperature, the green product filtered was washed with cold ethanol and petroleum ether to afford the target compound. Yield: 0.267 g (59%). ^{1}H NMR (400 MHz, CDCl$_3$): δ = 12.49(s, 2H, O*H*), 8.57（s, 2H, C*H*=N), 7.56(d, 2H, Ar-*H*), 6.43−6.46 (m, 2H, Ar-*H*), 6.16 (d, 2H, Ar-*H*), 3.32−3.47 (m, 8H, C*H*$_2$), 1.10−1.17 (m, 12H, C*H*$_3$) ppm. IR (KBr): $\tilde{\upsilon}$ = 2925(-C−H), 2868, 2350, 1617 (-C=N-), 1577, 1519, 1463, 1416, 1360, 1327, 1259, 1173, 1128, 1077 and 785 cm^{-1}. HRMS (MALDI-TOF, positive mode, CH$_2$Cl$_2$): m/z = 458.2412 [M+H]$^+$ (C$_{26}$H$_{30}$N$_6$O$_2^+$ H: calcd. 458.2425, Δ_m = 2.78 ppm). UV-Vis (CH$_2$Cl$_2$, 20°C): λ_{max} = 377, 437 and 571 nm. Luminescence (CH$_2$Cl$_2$, 20°C): λ_{max} = 612 nm. C$_{26}$H$_{30}$N$_6$O$_2$ (458.5554): calcd. C 68.10, H 6.59, N 18.33; found C 68.29 , H 6.64 , N. 18.11 .

H$_2$L^2 To a stirred solution of benzene-1,2-diamine (236 mg, 2.18 mmol) in absolute ethanol (20 mL), 4-(diethylamino)-2-hydroxybenzaldehyde (888 mg, 4.59 mmol) was added. The resulting mixture was refluxed 12 hours. After cooling to room temperature, the brown product precipitated was washed with cold ethanol and petroleum ether. Yield: 0.254 g (25%). ^{1}H NMR (400 MHz, CDCl$_3$): δ = 13.63（s, 2H, -O*H*), 8.42 (s, 2H, C*H*=N), 7.12-7.26 (m, 6H, Ar-*H*), 6.19-6.23 (m, 4H, Ar-*H*), 3.37 (q, 8H, -C*H*$_2$) and 1.19 (s, 12H, -C*H*$_3$) ppm. IR (KBr): $\tilde{\upsilon}$ = 2969 (-C-H), 2892, 2358, 1635 (-C=N-), 1598, 1517, 1507, 1457, 1352, 1239, 1132, 1077, 977 and 784 cm^{-1}. HRMS (MALDI-TOF, positive mode, CH$_2$Cl$_2$): m/z = 459.2799 [M+H]$^+$ (C$_{28}$H$_{34}$N$_4$O$_2$+H: calcd. 459.2754, Δ_m = 9.68 ppm). UV-Vis (CH$_2$Cl$_2$, 20 °C): λ_{max} = 241, 359 and 400nm. Luminescence (CH$_2$Cl$_2$, 20 °C): λ_{max} = 515 nm. C$_{28}$H$_{34}$N$_4$O$_2$ (458.5952): calcd. C 73.33, H 7.47, N 12.22; found C 73.21 , H 7.39, N 12.34 .

H$_2$L^3 To a stirred solution of 4-(trifluoromethyl)benzene-1,2-diamine (152 mg, 0.86 mmol) in absolute ethanol (20 mL), 3,5-di-tert-butyl-2-hydroxybenzaldehyde (606 mg, 2.59 mmol) was added. The resulting mixture was refluxed 12 hours. After cooling to room temperature, the orange product precipitated was washed with cold ethanol and petroleum ether. Yield: 0.315 g (60%). ^{1}H NMR (400 MHz, CDCl$_3$): δ = 13.28 (s, 1H, O*H*), 13.26 (s, 1H, O*H*), 8.72 (s, 1H, C*H*=N), 8.69 (s, 1H, C*H*=N), 7.60 (t, 1H, Ar-*H*), 7.49−7.50 (m, 3H, Ar-*H*), 7.25−7.34 (m, 3H, Ar-*H*), 1.35−1.59 (m, 36H, $\mathrm{C}H_3$) ppm. IR (KBr): ῦ = 2975 (-C−H), 2713, 2207, 1630 (-C=N-), 1564, 1508, 1482, 1436, 1341 (-$C(CH_3)_3$), 1231, 1204, 1186, 1135, 1078, 956, 827, 788 and 678 cm^{-1}. HRMS (MALDI-TOF, positive mode, CH_2Cl_2): m/z = 609.3610 $[M+H]^+$ ($C_{37}H_{47}F_3N_2O_2$+H: calcd. 609.3662, Δ_m = 8.53 ppm). UV-Vis (CH_2Cl_2, 20 °C): λ_{max} = 237, 285 and 334 nm. Luminescence (CH_2Cl_2, 20 °C): λ_{max} = 611 nm. $C_{37}H_{47}F_3N_2O_2$ (608.7765): calcd. C 73.00, H 7.78, N 4.60; found C 73.25 , H 7.64 , N 4.46 .

PtL^1 A solution of H_2L^1 (200 mg, 0.44 mmol), 2 equivalent of potassium hydroxide (49 mg, 0.88 mmol) were stirred about half an hour in 4ml DMF under nitrogen at 70℃. Then, potassium tetrachloroplatinate (II) (181 mg, 0.44 mmol) in DMSO (3 mL) were added to the solution for 24 h under nitrogen at 70℃. D. I. water was then added, the mixture was filtered extracted with $CHCl_3$ and dry in the vacuum. The crude product was purified by silica-gel column chromatography using a solvent mixture of hexane and $CHCl_3$ as eluent to give an dark-green solid of **PtL^1**. Yield: 113 mg (40%). ^{1}H NMR (400 MHz, $CDCl_3$): δ = 8.29 (s, 2H, C*H*=N), 7.71 (d, 2H, Ar-*H*), 6.56–6.59 (m, 2H, Ar-*H*), 6.30 (d, 2H, Ar-*H*), 3.35–3.53 (m, 8H, -$\mathrm{C}H_2$) and 1.13–1.24 (m, 12H, $\mathrm{C}H_3$) ppm. IR (KBr): ῦ = 2958(-C–H), 2871, 2357, 1616 (-C=N-), 1579, 1466, 1436, 1361, 1330, 1271, 1200, 1172, 1116, 1077, 929, 825 and 774 cm^{-1}. HRMS (MALDI-TOF, positive mode, CH_2Cl_2): m/z = 651.1994 $[M+H]^+$ ($C_{26}H_{28}N_6O_2Pt$: calcd. 651.1918, Δ_m = 1.19 ppm). $C_{26}H_{28}N_6O_2Pt$ (651.6235): calcd. C 47.92, H 4.33, N 12.90; found C 47.99, H 4.08, N 12.79.

PtL^2 A solution of H_2L^2 (220 mg, 0.48 mmol), 2 equivalent of potassium hydroxide (54 mg, 0.96mmol) were stirred about half an hour in 4ml DMF under nitrogen at 70℃. Then, potassium tetrachloroplatinate (II) (200 mg, 0.49 mmol) in DMSO (3 mL) were added to the solution for 24 h under nitrogen at 70℃. D. I. water was then added, the mixture was filtered extracted with $CHCl_3$ and dry in the vacuum. The crude product was purified by silica-gel column chromatography using a solvent mixture of hexane and $CHCl_3$ as eluent to give an red solid of **PtL^2**. Yield: 147 mg (47%). ^{1}H NMR (400 MHz, d^6-DMSO): δ = 8.98 (s, 2H，C*H*=N), 8.25 (s, 2H, Ar-*H*), 7.55 (d, 2H, Ar-*H*) , 7.25 (s, 2H, Ar-*H*), 6.37 (d, 2H, Ar-*H*), 6.17(s, 2H, Ar-*H*), 3.42 (q, 8H, -$\mathrm{C}H_2$) and 1.17 (t, 12H, -$\mathrm{C}H_3$) ppm. IR (KBr): ῦ = 2969(-C–H), 2921, 2350, 1616 (-C=N-), 1597, 1560, 1490, 1351, 1250, 1198, 1141, 1078, 816 and 751 cm^{-1}. HRMS (MALDI-TOF, positive mode, CH_2Cl_2): m/z = 652.2280 $[M+H]^+$ ($C_{28}H_{32}N_4O_2Pt$+H: calcd. 652.2248, Δ_m = 4.88 ppm). $C_{28}H_{32}N_4O_2Pt$ (651.6633): calcd. C 51.61, H 4.95, N 8.60; found C 51.02, H 4.99, N. 8.78.

PtL^3 A solution of H_2L^3 (200 mg, 0.33 mmol), 2 equivalent of potassium hydroxide (37 mg, 0.66 mmol) were stirred about half an hour in 4ml DMF under nitrogen at 70℃. Then, potassium tetrachloroplatinate (II) (137 mg, 0.33 mmol) in DMSO (3 mL) were added to the solution for 24 h under nitrogen at 70℃. D. I. water was then added, the mixture was filtered extracted with $CHCl_3$ and dry in the vacuum. The crude product was purified by silica-gel column chromatography using a solvent mixture of hexane and $CHCl_3$ as eluent to give black solid of **PtL^3**. Yield: 105 mg (40%). ^{1}H NMR (400 MHz, $CDCl_3$): δ = 8.97 (s, 1H, C*H*=N), 8.95 (s, 1H, C*H*=N), 8.28(s, 1H, Ar-*H*), 8.15 (d, 1H, Ar-*H*), 7.73 (s, 2H, Ar-*H*), 7.59 (d, 1H, Ar-*H*), 7.39 (d, 2H, Ar-*H*), 1.28−1.61 (m, 36H, $\mathrm{C}H_3$) ppm. IR (KBr): ῦ = 2974 (-C–H), 2920, 2214, 1616 (-C=N-), 1569, 1551, 1516, 1475, 1413, 1375 (-$C(CH_3)_3$), 1354, 1306, 1224, 1187, 1143, 107, 821 and 742 cm^{-1}. HRMS (MALDI-TOF, positive mode, CH_2Cl_2): m/z = 802.3121 $[M+H]^+$ ($C_{37}H_{45}F_3N_2O_2Pt$+H: calcd. 802.3157, Δ_m = 4.49 ppm). $C_{37}H_{45}F_3N_2O_2Pt$ (801.8446): calcd. C 55.42, H 5.66, N 3.49; found C 55.81, H 5.88, N. 3.21.

Acknowledgements

This work was supported by the Zhejiang Provincial Natural Science Foundation of China (No. LQ13B010001), National Natural Science Foundation of China(No. 21501128, 21375092, 21203135), China Postdoctoral Science Foundation (No. 2014M560476) and Key Disciplines of Applied Chemistry of Zhejiang Province, Taizhou University. We also thank the Project of Science and Technology Innovation for College Students in Zhejiang Province(No.2014R428016), Natural Science Fund for Colleges and Universities in Jiangsu Province (No. 14KJB150024) and Scientific Research Founding of Wuhan Institute of Technology (No. K201542) for financial support. X. Zhu thanks the financial support from Hong Kong Baptist University (FRG2/14-15/034 and FRG1/14-15/058).

References

[1] (a) Y. Hai, J. J. Chen, P. Zhao, H. B. Lv, Y. Yu, P. Y. Xu, J. L. Zhang *Chem. Commun.,* **2011**, *47*, 2435-2437; (b) F. Gao, L. Cui, W. Liu, L. Hu, Y. W. Zhong, Y. Z. Li, J. L. Zuo, *Inorg. Chem.,* **2013**, *52*, 11164-11172; (c) Z. Zhang, W. X. Peng, P. Y. Su, X. Q. Lu, J. R. Song, D. Fan, W. K. Wong, R. A. Jones, C. Y. Su, *Inorg. Chem.,* **2014**, *53*, 5950-5960; (d) M. Nematirad, W. J. Gee, S. K. Langley, N. F. Chilton, B. Moubaraki, K. S. Murray, S. R. Batten, *Dalton Trans.,* **2012**, *41*, 13711-13715.

[2] (a) S. S. Zhao, X. R. Liu, W. Y. Wong, X. Q. Lu, W. K. Wong, *Inorg. Chim. Acta,* **2014**, *414*, 160-164; (b) M. Kuil, I. M. Puijk, A. W. Kleij, D. M. Tooke, A. L. Spek, J. N. H. Reek, *Chem. Asian J.,* **2009**, *4*, 50-57; (c) A. W. Kleij, *Eur. J. Inorg. Chem.,* **2009**, 193-205.

[3] (a) J. Zhang, C. Zhong, X. J. Zhu, H. L. Tam, K. F. Li, K. W. Cheah, W. Y. Wong, W. K. Wong, R. A. Jones, *Polyhedron,* **2013**, *49*, 121-128; (b) J. Zhang, M. Y. Teng, G. L. Dai, S. L. Zhao, J. L. Wang, P. Zhang, T. T. Song, *Chinese J. Inorg. Chem.,* **2014**, *30*, 499-505.

[4] (a) B. H. Zhang, G. P. Tan, C. S. Lam, B. Yao, C. L. Ho, L. H. Liu, Z. Y. Xie, W. Y. Wong, J. Q. Ding, L. X. Wang, *Adv. Mater.,* **2012**, *24*, 1873-1877; (b) M. C. Tang, D. P. K. Tsang, M. M. Y. Chan, K. M. C. Wong, V. W. W. Yam, *Angew Chem. Int. Edit.,* **2013**, *52*, 446-449; (c) X. S. Xiao, W. L. Kwong, X. G. Guan, C. Yang, W. Lu, C. M. Che, *Chem. Eur. J.,* **2013**, *19*, 9457-9462.

[5] (a) Y. H. Zheng, A. S. Batsanov, M. A. Fox, H. A. Al-Attar, K. Abdullah, V. Jankus, M. R. Bryce, A. P. Monkman, *Angew Chem. Int. Edit.,* **2014**, *53*, 11616-11619; (b) J. Jayabharathi, V. Thanikachalam, R. Sathishkumar, *New J. Chem.,* **2015**, *39*, 235-245; (c) Q. Wang, D. G. Ma, K. Leo, J. Q. Ding, L. X. Wang, Q. Q. Qiao, H. P. Jia, B. E. Gnade, *Appl. Phys. Lett.,* **2014**, *104*; (d) H. T. Cao, G. G. Shan, Y. M. Yin, H. Z. Sun, Y. Wu, W. F. Xie, Z. M. Su, *Dyes Pigments,* **2015**, *112*, 8-16; (e) C. O. Paul-Roth, S. Drouet, A. Merhi, J. A. G. Williams, L. F. Gildea, C. Pearson, M. C. Petty, *Tetrahedron,* **2013**, *69*, 9625-9632.

[6] (a) M. A. Baldo, M. E. Thompson, S. R. Forrest, *Nature* **2000**, *403*, 750-753; (b) P. K. Chow, C. S. Ma, W. P. To, G. S. M. Tong, S. L. Lai, S. C. F. Kui, W. M. Kwok, C. M. Che, *Angew Chem. Int. Edit.* **2013**, *52*, 11775-11779.

[7] (a) F. Galbrecht, X. H. Yang, B. S. Nehls, D. Neher, T. Farrell, U. Scherf, *Chem. Commun.* **2005**, 2378-2380; (b) C. M. Che, S. C. Chan, H. F. Xiang, M. C. W. Chan, Y. Liu, Y. Wang, *Chem. Commun.,* **2004**, 1484-1485; (c) C. M. Che, C. C. Kwok, S. W. Lai, A. F. Rausch, W. J. Finkenzeller, N. Y. Zhu, H. Yersin, *Chem. Eur, J.,* **2010**, *16*, 233-247; (d) G. S. M. Tong, P. K. Chow, W. P. To, W. M. Kwok, C. M. Che, *Chem. Eur. J.,* **2014**, *20*, 6433-6443.

[8] J. Zhang, F. C. Zhao, X. J. Zhu, W. K. Wong, D. G. Ma, W. Y. Wong, *J. Mater. Chem.,* **2012**, *22*, 16448-16457.

[9] L. A. Duan, J. A. Qiao, Y. D. Sun, Y. Qiu, *Adv. Mater.,* **2011**, *23*, 1137-1144.

[10] W. K. Lo, W. K. Wong, W. Y. Wong, J. P. Guo, K. T. Yeung, Y. K. Cheng, X. P. Yang, R. A. Jones, *Inorg. Chem.,* **2006**, *45*, 9315-9325.

[11]Z. Asadi, M. Asadi, A. Zeinali, M. Ranjkeshshorkaei, K. Fejfarova, V. Eigner, M. Dusek, A. Dehnokhalaji, *J. Chem. Sci.*, **2014**, *126*, 1673–1683.

[12] Z. W. Liu, Z. Q. Bian, F. Hao, D. B. Nie, F. Ding, C. H. Huang, *Org. Electron.,* **2009**, *10*, 247-255.

[13] A. D. Becke, *J. Chem. Phys.,* **1993**, 98,1372-1377.

[14] M. Dolg, H. Stoll, H. Preuss, *Theor. Chim. Acta.,* **1993**, *85*, 441-450; (b) M. Dolg, H. Stoll, A. Savin, H. Preuss, *Theor. Chim. Acta.,* **1989**, *75*, 173-194.

[15] M. J. Frisch, et al. Gaussian 03, Revision B04, Gaussian Inc., Pittsburgh PA, **2003**.

[16] A. E. Reed, L. A. Curtiss, F. Weinhold, *Chem. Rev.,* **1988**, *88*, 899- 926.

Figure Captions

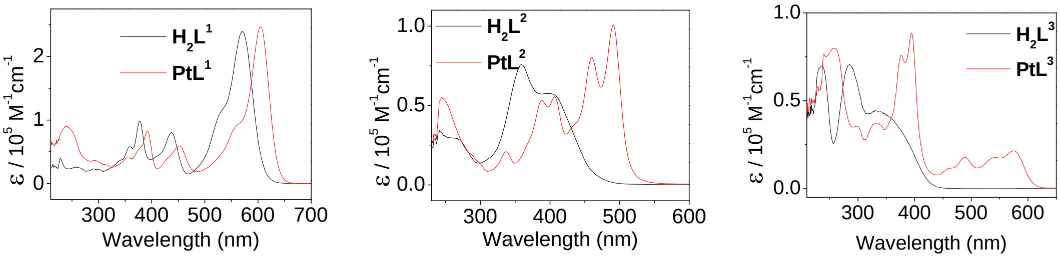

Figure 1. UV-visible absorption spectra of the Schiff base ligands and their corresponding platinum(II) complexes in DCM (1.0×10^{-5} M).

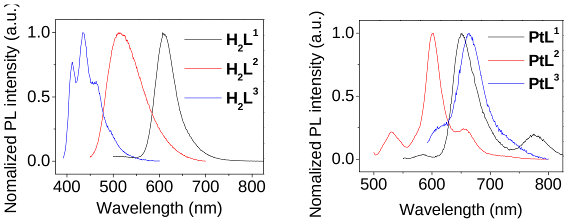

Figure 2. Emission spectrum of Schiff base ligands (left) and complexes (right) in DCM (1.0×10^{-5} M).

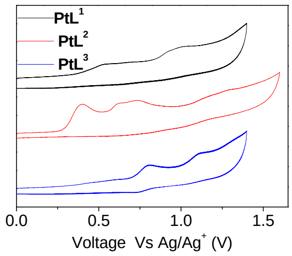

Figure 3. Cyclic voltammogram of the complexes.

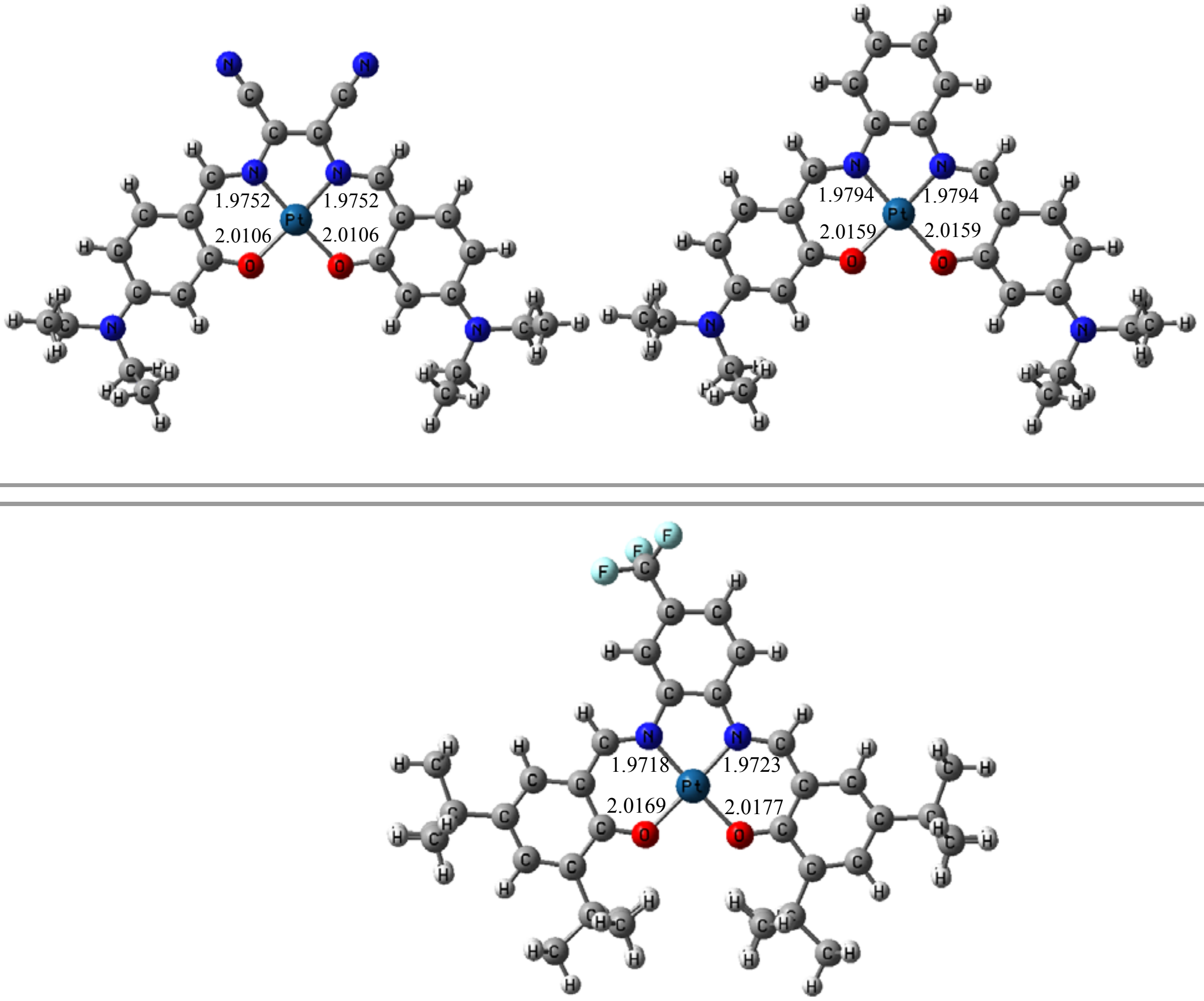

Figure 4. Optimized geometry of **PtL^1**, **PtL^2** and **PtL^3**; Bond lengths (Å) are written on the figure; dihedral angle were shown in **Figure S6-S8 (ESI)**.

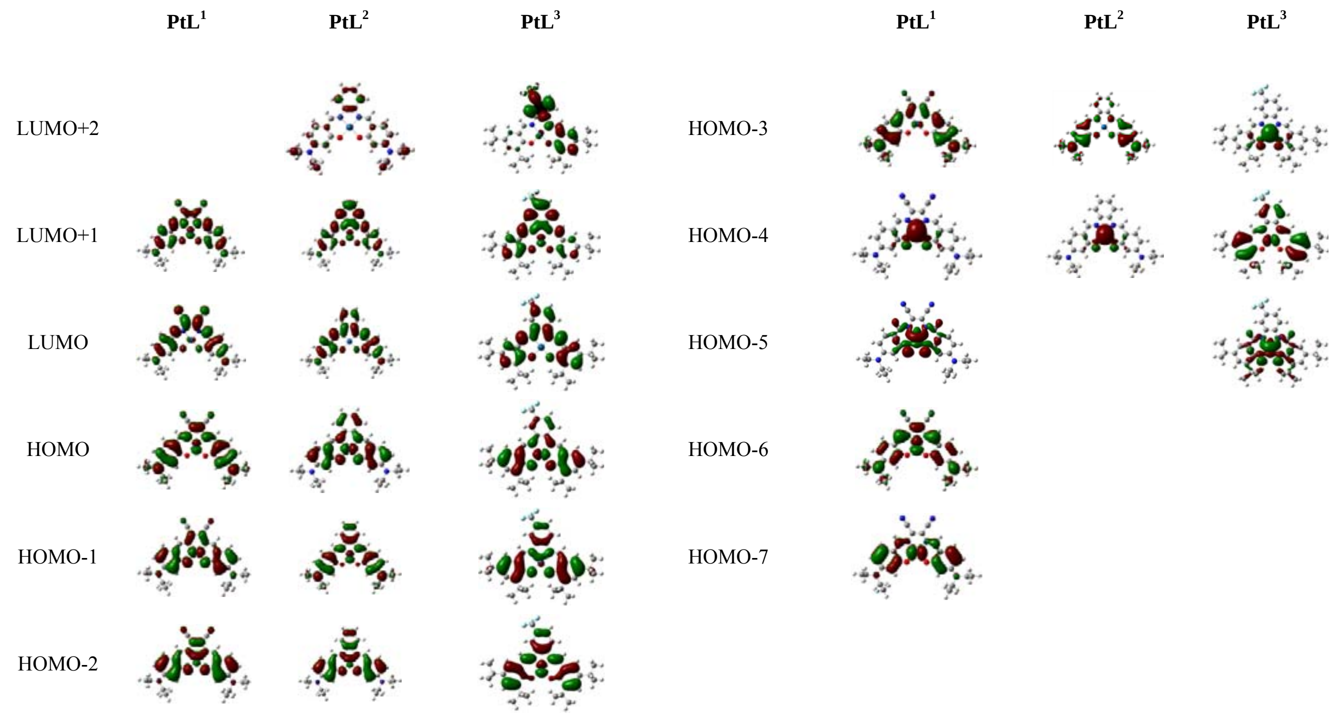

Figure 5. The frontier molecular orbitals of **PtL^1**, **PtL^2** and **PtL^3**.

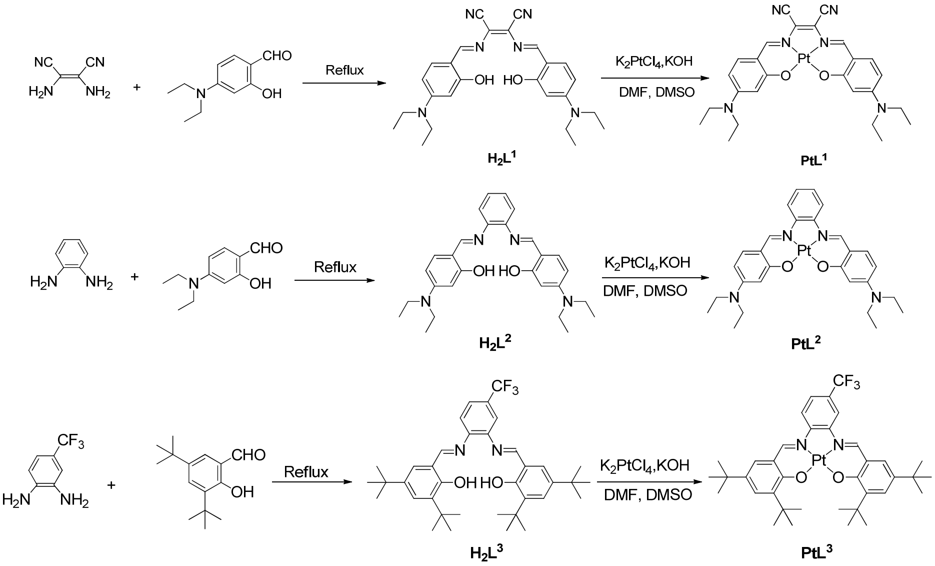

Scheme 1. The synthetic routes for the Schiff-base ligand **H_2L^1**, **H_2L^2** and **H_2L^3** and their platinum(II) complexes **PtL^1**, **PtL^2** and **PtL^3**.

Tables

Table 1. Summary of UV-visible absorption and luminescent data of complexes at room temperature in DCM (1.0×10^{-5} M).

Compd	Absorption λ_{max} (nm)^a	Luminescence λ_{max} (nm)	Φ_{em}^{b} (%)	τ (μs)	K_r ($\times10^3$ s^{-1})^c	K_{nr} ($\times10^3$ s^{-1})^d
H_2L^1	378,437,571	607	-	-	-	-
H_2L^2	241, 359, 400	511	-	-	-	-
H_2L^3	237, 285, 334	412, 435	-	-	-	-
PtL^1	393, 453, 607	650,776	8.6	1.97	43.7	463.9
PtL^2	244, 336, 389, 407, 461, 491	531, 601, 654	4.4	1.82	24.2	525.3
PtL^3	376, 396, 458, 491, 575	664	0.87	2.35	3.7	421.8

[a] Photophysical measurements were made with a concentration of 1×10^{-5} M in CH_2Cl_2 at room temperature. [b] Luminescence quantum yields (Φ_{em}) in degassed dichloromethane solution were determined with $[Ru(bpy)_3](PF_6)_2$ (bpy = 2,2'-bipyridine) in acetonitrile as a standard reference solution (Φ_{em} = 0.062) and 450 nm as excitation wavelength. [c] Radiative rate constants K_r was calculated from the value of Φ_{em}/τ. [d] Non-radiative rate constants K_{nr} was calculated from the equation of $\tau = (K_r + K_{nr})^{-1}$.

Table 2. Summary of cyclic voltammetry and TGA data.

Compound	E_{ox}	HOMO[a]	LUMO[b]	E_{gap}[c]	T_d (ºC)
PtL^1	0.35	-5.06	-3.28	1.78	352
PtL^2	0.29	-5.00	-2.89	2.11	340
PtL^3	0.71	-5.42	-3.50	1.92	350

[a] Estimated from the oxidation potentials HOMO = $-(E_{ox} + 4.71)$ eV . [b] Deduced from the HOMO and E_{gap}. [c] Estimated from the UV-vis absorption spectra.

Table 3. Theoretical results of major transition (percentage), transition energies (*E*), oscillator strengths (*f*) of **PtL^1**, **PtL^2** and **PtL^3**.

Singlet excited state	Major transition	*E*(nm)	*f*
PtL^1			
S1	HOMO-1→LUMO(67%)	550.23	0.0254
S2	HOMO→LUMO(62%)	541.17	0.6368
S3	HOMO-2→LUMO(65%)	479.74	0.1676
S4	HOMO-4→LUMO(70%)	433.66	0.0000
S5	HOMO-3→LUMO(65%)	427.54	0.1603
S6	HOMO-5→LUMO(70%)	374.26	0.0000
S7	HOMO-1→LUMO+1(67%)	364.38	0.0001
S8	HOMO→LUMO+1(68%)	351.27	0.1836
S9	HOMO-6→LUMO(61%)	337.96	0.0124
S10	HOMO-7→LUMO(68%)	333.89	0.1758
PtL^2			
S1	HOMO→LUMO(68%)	506.03	0.0447
S2	HOMO-1→LUMO(58%)	448.46	0.4580
S3	HOMO→LUMO+1(58%)	434.34	0.3710
S4	HOMO-2→LUMO(68%)	411.86	0.0003
S5	HOMO-1→LUMO+1(61%)	397.78	0.0652
S6	HOMO-4→LUMO(71%)	383.52	0.0000
S7	HOMO-3→LUMO(53%)	373.06	0.2410
S8	HOMO-4→LUMO+1(60%)	345.80	0.0987
S9	HOMO-2→LUMO+1(58%)	345.64	0.3034
S10	HOMO-3→LUMO+1(69%)	341.37	0.0893
PtL^3			
S1	HOMO→LUMO(67%)	558.09	0.0676
S2	HOMO→LUMO+1(68%)	471.00	0.0123
S3	HOMO-1→LUMO(68%)	466.81	0.0261
S4	HOMO-3→LUMO(70%)	396.58	0.0000
S5	HOMO-1→LUMO+1(66%)	389.38	0.1528
S6	HOMO-2→LUMO(66%)	384.28	0.5815
S7	HOMO-5→LUMO(70%)	355.60	0.0000
S8	HOMO-4→LUMO (63%)	352.58	0.0126
S9	HOMO-3→LUMO+1(69%)	350.40	0.0002
S10	HOMO-2→LUMO+1(62%)	342.73	0.1105